Inorg. Chem. **2006**, *45*, 9974–9984

Forum

Incorporating Electron-Transfer Functionality into Synthetic Metalloproteins from the Bottom-up

Jing Hong, Olesya A. Kharenko, and Michael Y. Ogawa*

Department of Chemistry and Center for Photochemical Sciences, Bowling Green State University, Bowling Green, Ohio 43403

Received February 8, 2006

The α-helical coiled-coil motif serves as a robust scaffold for incorporating electron-transfer (ET) functionality into synthetic metalloproteins. These structures consist of a supercoiling of two or more α helices that are formed by the self-assembly of individual polypeptide chains whose sequences contain a repeating pattern of hydrophobic and hydrophilic residues. Early work from our group attached abiotic Ru-based redox sites to the most surface-exposed positions of two stranded coiled-coils and used electron-pulse radiolysis to study both intra- and intermolecular ET reactions in these systems. Later work used smaller metallopeptides to investigate the effects of conformational gating within electrostatic peptide–protein complexes. We have recently designed the C16C19-GGY peptide, which contains Cys residues located at both the "a" and "d" positions of its third heptad repeat in order to construct a nativelike metal-binding domain within its hydrophobic core. It was shown that the binding of both Cd(II) and Cu(I) ions induces the peptide to undergo a conformational change from a disordered random coil to a metal-bridged coiled-coil. However, whereas the Cd(II)–protein exists as a two-stranded coiled-coil, the Cu(I) derivative exists as a four-stranded coiled-coil. Upon the incorporation of other metal ions, metal-bridged peptide dimers, tetramers, and hexamers are formed. The Cu(I)–protein is of particular interest because it exhibits a long-lived (microsecond) room-temperature luminescence at 600 nm. The luminophore in this protein is thought to be a multinuclear Cu^{I}_{4}-$Cys_4(N/O)_4$ cage complex, which can be quenched by exogenous electron acceptors in solution, as shown by emission-lifetime and transient-absorption experiments. It is anticipated that further investigation into these systems will contribute to the expanding effort of bioinorganic chemists to prepare new kinds of functionally active synthetic metalloproteins.

Introduction

Metalloproteins comprise approximately one-third of all structurally characterized proteins and perform such important biochemical functions as the catalytic transformation of chemical substrates, the facilitation of redox-dependent chemical reactions, and the mediation of oxygen transport and storage. The diversity of chemical functions performed by naturally occurring metalloproteins has inspired recent work toward the design of artificial analogues that might possess activities that mimic, enhance, or even replace those now performed by native systems.[1−7] However, this goal now presents a formidable challenge to the scientific community because it requires not only the ability to construct well-defined protein structures that can bind specific kinds of metal ions but also the ability to do so in ways that exploit the inherent chemical reactivity of these ions in order to incorporate tailorable chemical functions into these systems.

In general, two complementary approaches have been taken to synthesize new types of chemically functional

* To whom correspondence should be addressed. E-mail: mogawa@bgsu.edu.

(1) Gilardi, G.; Fantuzzi, A. *Trends Biotechnol.* **2001**, *19*, 468−476.
(2) Barker, P. D. *Curr. Opin. Struct. Biol.* **2003**, *13*, 490−499.
(3) Wittung-Stafshede, P. *Acc. Chem. Res.* **2002**, *35*, 201−208.
(4) Xing, G.; DeRose, V. J. *Curr. Opin. Chem. Biol.* **2001**, *5*, 196−200.
(5) Lu, Y.; Berry, S. M.; Pfister, T. D. *Chem. Rev.* **2001**, *101*, 3047−3080.
(6) Kennedy, M. L.; Gibney, B. R. *Curr. Opin. Struct. Biol.* **2001**, *11*, 485−490.
(7) Baltzer, L.; Nilsson, J. *Curr. Opin. Biotechnol.* **2001**, *12*, 355−360.

10.1021/ic060222j CCC: $33.50
Published on Web 12/04/2006

metalloproteins. The "top-down" approach refers to the reengineering of native proteins in ways that enable them to perform new chemical tasks that can be significantly different from their inherent biological functionality.[2,5,8,9] Alternatively, the "bottom-up" strategy refers to the rational assembly of discrete peptidic and inorganic building blocks in ways that can create synthetic protein structures whose inorganic components can perform interesting chemical reactions. To date, most work in the field of "bottom-up" metalloprotein design has concentrated on the essential, albeit preliminary, task of developing native-like peptide scaffolds that can bind specific metal ions. Notable examples of these include the designed metalloprotein in which two self-associated helix−loop−helix units are used to bind two separate iron atoms,[10−13] the bridged $Ni^{II}(\mu_2\text{-SCys})[Fe_4S_4]$ protein in which the helix−loop−helix motif creates a bridged metal-binding site,[14] several series of Cys-containing helical bundle proteins,[15−28] and the well-studied four-helix bundle heme proteins.[29]

Pecoraro and co-workers[15−23] have been conducting an elegant series of studies to examine the metal-binding properties of an important family of coiled-coil peptides prepared by subtle modifications of the parent peptide known as "TRI". TRI has the sequence Ac-G(LKALEEK)$_4$G-NH$_2$, which places hydrophobic leucine residues at each of the heptad "a" and "d" positions of an α-helical coiled-coil (vida infra) and was found to exist predominately as a three-stranded coiled-coil at pH > 7. Importantly, it was observed that the single replacement of one leucine residue with a Cys at either position 9 or 12 of the sequence created a metal-binding site having an affinity for Hg(II) and Cd(II) and that the resulting metallopeptides existed as three-stranded coiled-coils containing a very unusual three-coordinate metal center. This unexpected assembly process was seen to occur even in the case of a truncated peptide, which exists as a largely disordered coiled-coil in the absence of a metal ion. The results suggested that an important relationship exists between the conformational preferences of the apopeptide backbone and the coordination chemistry of the incorporated metal ion. Careful thermodynamic studies confirmed the existence of this relationship by showing a linear free-energy relationship between the self-association affinities of the TRI peptides and their ability to bind Hg(II) and Cd(II) ions in trigonal geometries.[15] These studies proved that, within the TRI family of metalloproteins, the conformational preferences of the protein dictate the coordination geometry of the incorporated metal ion.

Building upon recent successes in the "bottom-up" design of new metal-binding proteins, several workers have now begun to address the significant challenge of incorporating chemical functionality into these systems.[7] In a notable effort, DeGrado and co-workers recently prepared a computationally designed metalloprotein that has a diiron cluster, similar to those found in a variety of naturally occurring hydrolytic enzymes, positioned in close proximity to a suitable substrate-binding domain.[10−13] Significantly, this protein called DFtet was shown to catalyze the two-electron oxidation of 4-aminophenol to the corresponding quinone monoamine with a somewhat modest but distinct value of $k_{cat}/K_M = 1500\ M^{-1}\ min^{-1}$.[13] In related efforts, workers have successfully constructed chimeric metalloproteins that contain both the helix−turn−helix DNA binding domain and either the metal-binding loop of calmodulin[30,31] or an unnatural amino acid based on triazacyclononane[32] in order to bind hydrolytic metal ions. Such systems have been shown to display sequence-specific nuclease activity. Most recently, Dutton and co-workers have introduced the design of new amphiphilic heme protein maquettes (minimalistic protein models) in order to facilitate their incorporation of hydrophobic cofactors in a manner that mimics native photosynthetic proteins.[33−35] Thus, significant achievements in functional metalloprotein design have begun to appear through

(8) Bloom, J. D.; Meyer, M. M.; Meinhold, P.; Otey, C. R.; MacMillan, D.; Arnold, F. H. *Curr. Opin. Struct. Biol.* **2005**, *15*, 447−452.
(9) Dwyer, M. A.; Looger, L. L.; Hellinga, H. W. *Science* **2004**, *304*, 1967−1971.
(10) Calhoun, J. R.; Nastri, F.; Maglio, O.; Pavone, V.; Lombardi, A.; DeGrado, W. F. *Biopolymers* **2005**, *80*, 264−278.
(11) Lombardi, A.; Summa, C. M.; Geremia, S.; Randaccio, L.; Pavone, V.; DeGrado, W. F. *Proc. Natl. Acad. Sci. U.S.A.* **2000**, *97*, 6298−6305.
(12) Maglio, O.; Nastri, F.; Pavone, V.; Lombardi, A.; DeGrado, W. F. *Proc. Natl. Acad. Sci. U.S.A.* **2003**, *100*, 3772−3777.
(13) Kaplan, J.; DeGrado, W. F. *Proc. Natl. Acad. Sci. U.S.A.* **2004**, *101*, 11566−11570.
(14) Laplaza, C. E.; Holm, R. H. *J. Am. Chem. Soc.* **2001**, *123*, 10255−10264.
(15) Ghosh, D.; Lee, K. H.; Demeler, B.; Pecoraro, V. L. *Biochemistry* **2005**, *44*, 10732−10740.
(16) Ghosh, D.; Pecoraro, V. L. *Inorg. Chem.* **2004**, *43*, 7902−7915.
(17) Lee, K. H.; Matzapetakis, M.; Mitra, S.; Neil, E.; Marsh, G.; Pecoraro, V. L. *J. Am. Chem. Soc.* **2004**, *126*, 9178−9179.
(18) Farrer, B. T.; Pecoraro, V. L. *Proc. Natl. Acad. Sci. U.S.A.* **2003**, *100*, 3760−3765.
(19) Matzapetakis, M.; Farrer, B. T.; Weng, T. C.; Hemmingsen, L.; Penner-Hahn, J. E.; Pecoraro, V. L. *J. Am. Chem. Soc.* **2002**, *124*, 8042−8054.
(20) Farrer, B. T.; Pecoraro, V. L. *Curr. Opin. Drug Discovery Dev.* **2002**, *5*, 937−943.
(21) Farrer, B. T.; Harris, N. P.; Balchus, K. E.; Pecoraro, V. L. *Biochemistry* **2001**, *40*, 14696−14705.
(22) Dieckmann, G. R.; McRorie, D. K.; Lear, J. D.; Sharp, K. A.; DeGrado, W. F.; Pecoraro, V. L. *J. Mol. Biol.* **1998**, *280*, 897−912.
(23) Dieckmann, G. R.; McRorie, D. K.; Tierney, D. L.; Utschig, L. M.; Singer, C. P.; Ohalloran, T. V.; PennerHahn, J. E.; DeGrado, W. F.; Pecoraro, V. L. *J. Am. Chem. Soc.* **1997**, *119*, 6195−6196.
(24) Tanaka, T.; Mizuno, T.; Fukui, S.; Hiroaki, H.; Oku, J.; Kanaori, K.; Tajima, K.; Shirakawa, M. *J. Am. Chem. Soc.* **2004**, *126*, 14023−14028.
(25) Kiyokawa, T.; Kanaori, K.; Tajima, K.; Koike, M.; Mizuno, T.; Oku, J. I.; Tanaka, T. *J. Pept. Res.* **2004**, *63*, 347−353.
(26) Li, X. Q.; Suzuki, K.; Kanaori, K.; Tajima, K.; Kashiwada, A.; Hiroaki, H.; Kohda, D.; Tanaka, T. *Protein Sci.* **2000**, *9*, 1327−1333.
(27) Kharenko, O. A.; Ogawa, M. Y. *J. Inorg. Biochem.* **2004**, *98*, 1971−1974.
(28) Kharenko, O. A.; Kennedy, D. C.; Demeler, B.; Maroney, M. J.; Ogawa, M. Y. *J. Am. Chem. Soc.* **2005**, *127*, 7678−7679.
(29) Reedy, C. J.; Gibney, B. R. *Chem. Rev.* **2004**, *104*, 617−649.
(30) Welch, J. T.; Kearney, W. R.; Franklin, S. J. *Proc. Natl. Acad. Sci. U.S.A.* **2003**, *100*, 3725−3730.
(31) Kovacic, R. T.; Welch, J. T.; Franklin, S. J. *J. Am. Chem. Soc.* **2003**, *125*, 6656−6662.
(32) Rossi, P.; Tecilla, P.; Baltzer, L.; Scrimin, P. *Chem.−Eur. J.* **2004**, *10*, 4163−4170.
(33) Discher, B. A.; Noy, D.; Strzalka, J.; Ye, S. X.; Moser, C. C.; Lear, J. D.; Blasie, J. K.; Dutton, P. L. *Biochemistry* **2005**, *44*, 12329−12343.
(34) Noy, D.; Discher, B. A.; Rubtsov, I. V.; Hochstrasser, R. A.; Dutton, P. L. *Biochemistry* **2005**, *44*, 12344−12354.
(35) Ye, S. X.; Discher, B. M.; Strzalka, J.; Xu, T.; Wu, S. P.; Noy, D.; Kuzmenko, I.; Gog, T.; Therien, M. J.; Dutton, P. L.; Blasie, J. K. *Nano Lett.* **2005**, *5*, 1658−1667.

the simultaneous incorporation of both metal- and substrate-binding centers into a single protein environment. It is anticipated that future study of these systems will provide considerable insight into how protein environments can be used to regulate the chemical reactivity of their incorporated transition-metal ions.

Aside from catalytic functionality, redox activity is another type of chemical property that can be incorporated into designed metalloproteins. Indeed, a long-standing effort to understand how protein structures can provide pathways for long-range donor−acceptor interactions has led to the development of many peptide-based electron-transfer (ET) reagents built from the "bottom-up". Early work in this field largely concentrated on the attachment of exogenous abiotic redox centers, such as ruthenium polypyridyl complexes, to polypeptide spacers possessing defined secondary structures such as proline helices and α helices. Such work has been the focus of a previous review.[36] However, more recent work in this field has resulted in the design of systems that can indeed be classified as examples of functionally active ET proteins having well-defined tertiary and/or quarternary structures, some with more nativelike redox cofactors.[37−42] In a notable example of such work, Haehnel and co-workers have been studying a family of modular four-helix, template-assembled synthetic proteins that are amenable to the incorporation of both metalloporphyrin[43] and chlorophyll[44] cofactors. Recent work by this group also involved the combinatorial assembly of Cu(II)-binding sites, which led to the creation of a mixed-valent dinuclear Cu site reminiscent of Cu_A.[45] The work described below will review our efforts to utilize the α-helical coiled-coil motif as a robust scaffold upon which inorganic redox centers can be either attached to their solvent-exposed surfaces or bound to nativelike binding sites designed within their hydrophobic cores.

Experimental Section

Materials. The Fmoc-protected L-amino acid derivatives, 2-(1*H*-benzotriazol-1-yl)-1,1,3,3-tetramethyluronium hexafluorophosphate, piperidine, diisopropylcarbodiimide, and anhydrous *N*-hydroxybenzotriazole were purchased from Peptides International Inc. (Louisville, KY). The reagent tetrakis(acetonitrile)copper(I) hexafluorophosphate was purchased from the Sigma-Aldrich Co. (St. Louis, MO). All reagents were used as received.

General Methods. UV−vis, circular dichroism (CD), and reversed-phase high-performance liquid chromatography (HPLC) analyses were performed as previously described[46] except that either a semipreparative Vydac reversed-phase 218TP C_{18} column (10 μM particle size, 10 × 250 mm) or a preparative Vydac 218TP C_{18} column (10 μM particle size, 22 × 250 mm) was used. Static luminescence spectra were obtained with a single-photon-counting spectrofluorimeter from Edinburgh Analytical Instruments (FL/FS 900), and emission-lifetime measurements were carried out using a nitrogen broad-band dye laser (2−3-nm full width at half-maximum) using fundamental nitrogen excitation (337 nm) or BPBD dye (357 nm) as previously decribed.[47] The emission of the Cu^I-C16C19-GGY adduct was monitored at 600 nm and performed in argon-saturated solutions.

Synthesis of the C16C19-GGY Peptide. The 32-residue peptide C16C19-GGY having the sequence Ac-K(IEALEGK)$_2$(CEACEGK)-(IEALEGK)-GGY-NH_2 was prepared and purified by reversed-phase HPLC as previously described.[48] The GGY tag was attached to the peptide to allow determination of the peptide concentration by measuring the absorption of the tyrosine residue at 275 nm (ϵ = 1450 M^{-1} cm^{-1}).[49]

High-Performance Size-Exclusion Chromatography (HPSEC). HPSEC experiments were performed using a Superdex 75 Biotech column (Amersham Biosciences) connected to a Waters model 515 HPLC pump equipped with a Waters model 996 diode-array detector. The peptide samples were eluted using 0.1 M KCl/0.05 M KH_2PO_4 with a 0.2−0.4 mL/min flow rate and monitored at 230 nm, and their behavior was compared against those of suitable peptide standards.[50]

Results and Discussion

Synthetic ET Metallproteins Based on α-Helical Coiled Coils. Our group has been preparing synthetic metalloproteins based on α-helical coiled-coils.[27,28,46,48,51−53] These ubiquitous structures comprise an important dimerization domain of native proteins and are formed by the noncovalent self-assembly of α helices. Such structures are stabilized by a specific "knobs into holes" packing of regularly spaced hydrophobic residues belonging to each strand of the coiled-coil. It has been found that synthetic coiled-coils can be prepared from amino acid sequences based on a seven-residue heptad repeat, $(abcdefg)_n$, in which hydrophobic amino acids occupy positions "a" and "d" of the heptad, hydrophilic residues fill positions "b", "c", and "f", and

(36) Ogawa, M. Y. In *Molecular and Supramolecular Photochemistry*; Ramamurthy, V., Schanze, K. S., Eds.; Marcel Dekker: New York, 1999; Vol. 4, pp 113−150.
(37) Zheng, Y. J.; Case, M. A.; Wishart, J. F.; McLendon, G. L. *J. Phys. Chem. B* **2003**, *107*, 7288−7292.
(38) Mutz, M. W.; Case, M. A.; Wishart, J. F.; Ghadiri, M. R.; McLendon, G. L. *J. Am. Chem. Soc.* **1999**, *121*, 858−859.
(39) Mutz, M. W.; McLendon, G. L.; Wishart, J. F.; Gaillard, E. R.; Corin, A. F. *Proc. Natl. Acad. Sci. U.S.A.* **1996**, *93*, 9521−9526.
(40) Kennedy, M. L.; Gibney, B. R. *J. Am. Chem. Soc.* **2002**, *124*, 6826−6827.
(41) Cristian, L.; Piotrowiak, P.; Farid, R. S. *J. Am. Chem. Soc.* **2003**, *125*, 11814−11815.
(42) Jones, G.; Vullev, V.; Braswell, E. H.; Zhu, D. *J. Am. Chem. Soc.* **2000**, *122*, 388−389.
(43) Fahnenschmidt, M.; Bittl, R.; Schlodder, E.; Haehnel, W.; Lubitz, W. *Phys. Chem. Chem. Phys.* **2001**, *3*, 4082−4090.
(44) Rau, H. K.; Snigula, H.; Struck, A.; Robert, B.; Scheer, H.; Haehnel, W. *Eur. J. Biochem.* **2001**, *268*, 3284−3295.
(45) Schnepf, R.; Haehnel, W.; Wieghardt, K.; Hildebrandt, P. *J. Am. Chem. Soc.* **2004**, *126*, 14389−14399.
(46) Kornilova, A. Y.; Wishart, J. F.; Xiao, W. Z.; Lasey, R. C.; Fedorova, A.; Shin, Y. K.; Ogawa, M. Y. *J. Am. Chem. Soc.* **2000**, *122*, 7999−8006.
(47) Tyson, D. S.; Castellano, F. N. *J. Phys. Chem. A* **1999**, *103*, 10955−10960.
(48) Fedorova, A.; Ogawa, M. Y. *Bioconjugate Chem.* **2002**, *13*, 150−154.
(49) Fasman, G. D. *Handbook of Biochemistry and Molecular Biology, Proteins, I*, 3rd ed.; CRC Press: Boca Raton, FL, 1976.
(50) Mant, C. T.; Chao, H.; Hodges, R. S. *J. Chromatogr. A* **1997**, *791*, 85−98.
(51) Kornilova, A. Y.; Wishart, J. F.; Ogawa, M. Y. *Biochemistry* **2001**, *40*, 12186−12192.
(52) Lasey, R. C.; Banerji, S. S.; Ogawa, M. Y. *Inorg. Chim. Acta* **2000**, *300−302*, 822−828.
(53) Fedorova, A.; Chaudhari, A.; Ogawa, M. Y. *J. Am. Chem. Soc.* **2003**, *125*, 357−362.

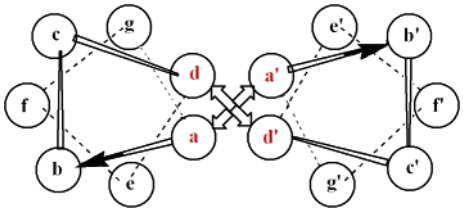

Figure 1. Helical wheel diagram depicting one heptad repeat of a two-stranded α-helical coiled-coil. The hydrophobic "a" and "d" positions are shown in red.

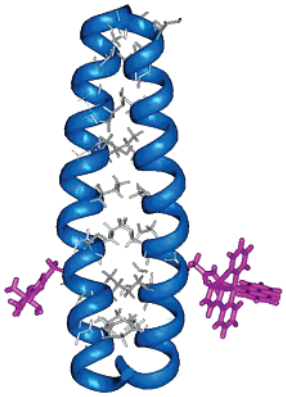

Figure 2. Computer-generated model of the synthetic ET protein formed by attaching Ru-based redox sites to His residues occupying the solvent-exposed "f" positions of a two-stranded coiled-coil.

oppositely charged residues may occupy positions "e" and "g" in order to form stabilizing interchain salt bridges (Figure 1).[54−57]

In early work, our group prepared a 30-residue polypeptide called H21(30-mer), whose sequence was designed to form two-stranded coiled-coils.[46] An important feature of the sequence

$$\text{Ac-K(IEALEGK)}_2\text{(IEALE}\underline{\mathbf{H}}\text{K)(IEALEGK)G-NH}_2$$

H21(30-mer)

is that it places a single His residue at position 21 to provide a convenient metal-binding site at the most highly solvent-exposed "f" position of the third heptad repeat. CD spectroscopy showed that this peptide did indeed exist as a α-helical coiled-coil in which the association process could be fit to a two-state monomer−dimer equilibrium having a value of $K_d = 1.5 \pm 0.4\ \mu$M and a maximum ellipticity of 69%. Treatment of the peptide with either $[Ru(NH_3)_5(OH_2)]^{2+}$ or $[Ru(trpy)(bpy)(OH_2)]^{2+}$ produced the corresponding metalated homodimers in which Ru compounds were coordinated to each of the two H21 sites of the coiled-coil. The desired ET heterodimer (Figure 2) was then prepared in a statistical distribution with the two metalated homodimers by heating an equimolar solution of the two metalated peptides to 60 °C and cooling the mixture back to room temperature. These peptides were shown by a combination of analytical ultracentrifugation, sodium dodecyl sulfate−polyacrylamide gel electrophoresis, and size-exclusion chromatography to exist as two-stranded coiled-coils. Importantly, electron paramagnetic resonance spin-labeling experiments were used to provide a measure of the interchain $C_\alpha - C_\alpha$ distance of 13.5 ± 0.9 Å at position 21 of the coiled-coil, which is nearly identical with those observed for the isostructural family of bZip proteins. These results enabled computer modeling studies to estimate that the two metal centers in the ET heterodimer were separated by a metal-to-metal distance of ca. 24 Å across the noncovalent peptide interface. Oxidative pulse radiolysis experiments were used to study intramolecular ET reactions occurring from the $Ru^{II}(NH_3)_5$-H21 donor to the Ru^{III}(trpy)(bpy)-H21′ acceptor located across the noncovalent peptide interface. The rate constant for the ET reaction was found to be $k_{ET} = 380\ s^{-1}$, which was independent of the peptide concentration. Significantly, these experiments showed that the observed rate constant is consistent with the distance-rate behavior observed in both native[58] and modified[59] protein systems and that intramolecular ET can indeed occur over long distances in this designed metalloprotein across a noncovalent peptide−peptide interface. The designed H21 metalloheterodimer is therefore a viable model system for natural ET proteins.

A Pathways[60] analysis was conducted for the H21(30-mer) system, which identified its primary coupling path (metal-to-metal) to consist of 22 covalent bonds and a critical interhelix through-space jump of 3 Å between the C_β of Lys22 and C_γ of Ile23′ of the next heptad repeat.[61] We therefore prepared a related peptide called H18(30-mer) whose metal-coordinating His residues were now located at position 18 of the sequence occupying the heptad "c" positions. It was hypothesized that this change should decrease the length of the putative ET tunneling pathway by three covalent bonds and increase the observed rate of intraprotein ET from the relatively slow rate observed for H21(30-mer). However, pulse radiolysis experiments showed no evidence for intraprotein ET occurring in this system, and only a concentration-dependent interprotein ET event was seen, having a second-order rate constant of k_{ET}(inter) $= 6 \times 10^8\ M^{-1}\ s^{-1}$. The reason for this disappointing result was explained by CD experiments, which showed that placement of the hydrophilic metal complexes closer to the noncovalent interface of this peptide resulted in destabilization of its coiled-coil structure. This likely led to an increased metal−metal distance in the H18(30-mer) metallopeptide to make its rate of intramolecular ET no longer competitive with that of the intermolecular reaction occurring between different proteins in the pulse radiolysis experiment.

ET along the Covalent Backbone of α Helices and Coiled Coils. Previous results by Fox and co-workers reported that the permanent dipole moment of α helices can be used to modulate the rates of photoinduced ET occurring

(54) Burkhard, P.; Stetefeld, J.; Strelkov, S. V. *Trends Cell Biol.* **2001**, *11*, 82−88.
(55) Kohn, W. D.; Hodges, R. S. *Trends Biotechnol.* **1998**, *16*, 379−389.
(56) Lupas, A. *Trends Biochem. Sci.* **1996**, *21*, 375−382.
(57) Hodges, R. S. *Biochem. Cell Biol.* **1996**, *74*, 133−154.
(58) Noy, D.; Moser, C. C.; Dutton, P. L. *Biochim. Biophys. Acta* **2006**, *1757*, 90−105.
(59) Winkler, J. R.; Di Bilio, A. J.; Farrow, N. A.; Richards, J. H.; Gray, H. B. *Pure Appl. Chem.* **1999**, *71*, 1753−1764.
(60) Wolfgang, J.; Risser, S. M.; Priyadarshy, S.; Beratan, D. N. *J. Phys. Chem. B* **1997**, *101*, 2986−2991.
(61) Kurnikov, I. Private communication.

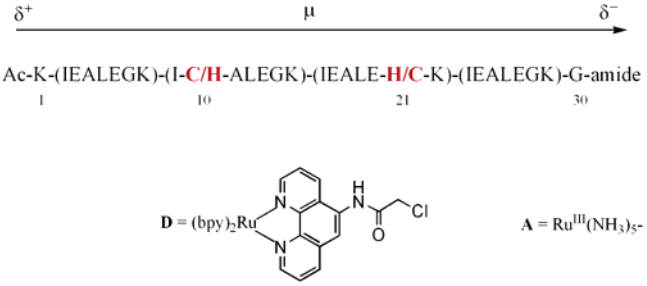

Figure 3. Sequence of the ET-I and ET-II in which the binuclear ET proteins were prepared by first reacting the ruthenium polypyridyl complex (D) to the Cys residue of the appropriate peptide and then attaching the pentaammineruthenium species (A) to the His residue.

between organic donors and acceptors.[62−64] Thus, our group designed a new peptide-based ET system to determine if this effect can also be used to regulate ET rates in metalloproteins.[48,53] Two 30-residue coiled-coil apopeptides were synthesized having the following sequences: (**I**) Ac-K-(IEALEGK)(ICALEGK)(IEALEHK)(IEALEGK)-G-NH_2 and (**II**) Ac-K-(IEALEGK)(IHALEGK)−(IEALECK)(IEALEGK)-G-NH_2 (Figure 3). Ru-based electron-donor and -acceptor sites were then attached to the Cys and His sites, respectively, to yield the binuclear ET metallopeptides ET-I and ET-II. Photoexcitation of the ruthenium polypyridyl donor resulted in ET occurring to the pentaammineruthenium(III) acceptor in a direction that was toward the negative end of the helix dipole in ET-I and the positive end in ET-II. Significantly, no evidence for directional ET rates was observed in these systems in aqueous solution, the low-dielectric solvent 2,2,2-trifluoroethanol (TFE), or a 1:1 (v/v) mixture of CH_2Cl_2−TFE. This behavior is in marked contrast to that observed for the systems studied by Fox and co-workers.[62−64] The reason for this apparent discrepancy is presently not understood. However, two important differences do exist between the two systems studied. First, the earlier work examined the rates of photoinduced ET occurring between nonpolar redox centers, but the peptides ET-I and ET-II employ charged, divalent and trivalent, metal complexes as their donor and acceptor sites. It is possible that the electrostatic effects generated by the presence of these charged complexes may supersede the effects exerted by the helix dipole. Second, the metallopeptide systems use a flexible acetyl linker to attach the ruthenium polypyridyl complex to the peptide chain, which can place this redox site at distances ranging from ca. 3 to 8 Å away from the helix axis (edge to backbone). This may also serve to reduce the effects of the helix dipole in regulating ET rates. Thus, to determine if these factors contribute to the absence of a helix-dipole effect, studies are currently underway to design systems that use redox sites that consist of neutral metal complexes, that do not require the use of an acetyl linker, and that can be placed at different regions of the sequence. As discussed below, work from our group has shown that a new family of

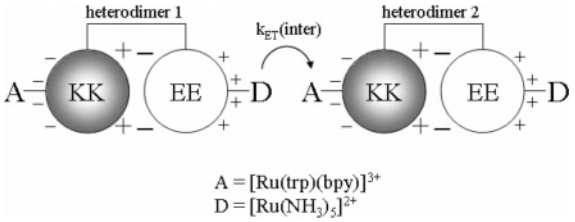

Figure 4. Schematic representation of the EE/KK electrostatic heterodimer emphasizing the charges on the solvent-exposed and interfacial regions of the heterodimer.

synthetic metalloproteins can be prepared in which redox-active cofactors can be buried within their hydrophobic interiors. Investigations of such systems may help elucidate the necessary requirements for allowing the helix-dipole moment to regulate ET rates in de novo designed metallopeptides and metalloproteins.

Gated ET To Study the Dynamics of Peptide−Protein Complexes. Our group's experience in preparing redox-active metallopeptides have been applied toward the study of ET processes that occur within electrostatic protein complexes. Early work in this project sought to understand how the incorporation of complementary electrostatic recognition domains onto the surface of coiled-coil metalloproteins can affect the rates of intermolecular ET occurring between separate metalloproteins.[51] Thus, interprotein ET reactions were studied that involve a $[Ru(NH_3)_5$-H21$]^{2+}$ electron donor and a [Ru(trpy)(bpy)-H21$]^{3+}$ electron acceptor that were embedded within protein surfaces having opposite charge: a $Ru^{II}(NH_3)_5$-H21 site was placed on the positive surface of a coiled-coil peptide, and a Ru^{III}(trpy)(bpy)-H21 site was placed on the negative surface of another peptide (Figure 4). No evidence for stable electrostatic complex formation was observed, and the rates of intermolecular ET were seen to follow bimolecular kinetics and *increase* from $k_{inter} = (1.9 \pm 0.4) \times 10^7$ to $(3.7 \pm 0.5) \times 10^7$ M^{-1} s^{-1} as the ionic strength was raised from 0.01 to 0.20 M. This somewhat unexpected result indicates that the electrostatic repulsion between the positively charged Ru centers dominates the kinetics of these reactions and not the complementary surface charges of the proteins. However, analysis by two different electrostatic models indicated that the presence of the oppositely charged protein surfaces in the coiled-coils does create an electrostatic recognition domain that substantially ameliorates the effects of this intermetal repulsion.

Encouraged by our ability to use electrostatic interactions to influence the rates of intermolecular ET reactions occurring between designed metalloproteins, we designed two small negatively charged metallopeptides capable of forming stable electrostatic complexes with ferricytochrome *c*. This work showed how the rates of intracomplex ET are gated by rate-limiting configurational changes occurring within the electrostatic peptide−protein complex.

Emission measurements showed that the triplet lifetime of the ruthenium metallopeptide, $[Ru(bpy)_2(phenam)Cys-(Glu)_5Gly]^{3-} = RuCE_5G$ (Figure 5), is shortened and decays via biexponential kinetics when in the presence of cytochrome *c* (Cyt *c*). These results indicate the existence of two excited-state populations of Ru−peptides, both of which

(62) Fox, M. A.; Galoppini, E. *J. Am. Chem. Soc.* **1997**, *119*, 5277−5285.
(63) Knorr, A.; Galoppini, E.; Fox, M. A. *J. Phys. Org. Chem.* **1997**, *10*, 484−498.
(64) Galoppini, E.; Fox, M. A. *J. Am. Chem. Soc.* **1996**, *118*, 2299−2300.

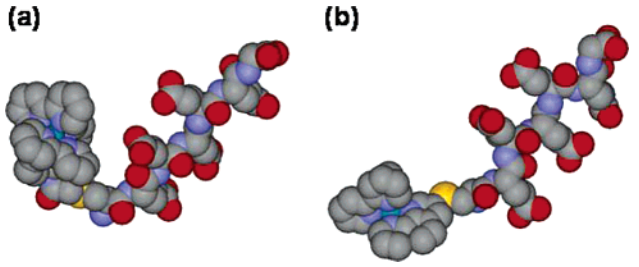

Figure 5. Energy-minimized structures of the metal−peptides (a) $RuCE_5G$ and (b) $RuCE_5G$-short, which differ by the method of attaching the Ru center to the Cys side chain.

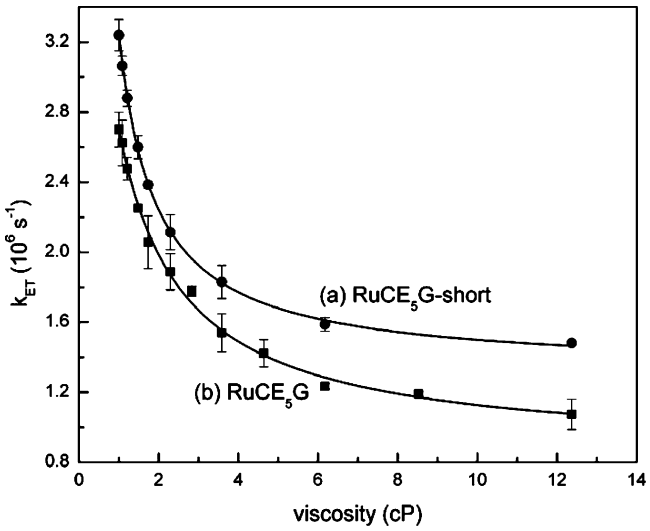

Figure 6. Viscosity dependence of intracomplex ET rate constants for (a) $RuCE_5G$-short and (b) $RuCE_5G$.

undergo photoinduced ET to the iron heme. The faster decay component displays concentration-independent kinetics, demonstrating the presence of a preformed peptide−protein complex, which undergoes intracomplex ET with a rate constant of $k_{ET}^{obs} = (2.7 \pm 0.4) \times 10^6$ s^{-1}. Significantly, the magnitude of k_{ET}^{obs} decreases with increasing solvent viscosity (Figure 6), and the behavior can be fit to the expression $k_{ET}^{obs} \propto \eta^{-\alpha}$ to give $\alpha = 0.59 \pm 0.05$. The ET process occurring in the preformed complex is *therefore gated by a rate-limiting configurational change of the complex*. The slower decay component displays concentration-dependent kinetics, which saturate at high concentrations of Cyt *c*. Analysis according to rapid equilibrium formation of an encounter complex, which then undergoes unimolecular ET, yields $k_{ET}^{obs\prime} = (7 \pm 3) \times 10^5$ s^{-1}. The smaller value of $k_{ET}^{obs\prime}$ suggests that a somewhat longer donor−acceptor distance exists in the encounter complex. Interestingly, the value of $k_{ET}^{obs\prime}$ is also viscosity-dependent, showing that this reaction is also gated. However, a value of $\alpha = 0.98 \pm 0.14$ was observed, which emphasized the very dynamic nature of the encounter complex.

Subsequent work demonstrated how a small modification of the metal−peptide could produce significant changes in the dynamics of its preformed complex.[65] Thus, a new example was prepared in which a ruthenium polypyridyl complex was coupled directly to the CE_5G peptide by reacting it with $[(bpy)_2Ru(3\text{-bromo-}1,10\text{-phenanthroline})](PF_6)_2$ to yield the compound $RuCE_5G$-short (Figure 5). This new metallopeptide differs from the original one only by the absence of the flexible acetyl linker joining the metal complex to the Cys side chain of the peptide. Photoinduced ET experiments showed that $RuCE_5G$-short also forms an electrostatic complex with Cyt *c*, within which intracomplex ET can occur. In addition, viscosity studies showed that this process is also gated by rate-limiting configurational changes of the complex. However, it was seen that the preformed complex involving $RuCE_5G$-short was more mobile ($\alpha = 0.97 \pm 0.03$) than the one involving the longer peptide (Figure 6) and had a higher binding constant. These observations were rationalized by molecular modeling studies, which indicated that the two peptides likely adopt different conformations (Figure 5). Whereas the short peptide has a roughly linear rodlike geometry, the flexible acetamido linker of $RuCE_5G$ allows it to form a hairpin-like structure in which the bulky ruthenium polypyridyl cation is placed in closer proximity to the negatively charged glutamate chain. It was speculated that the higher mobility of the $RuCE_5G$-short−Cyt *c* complex may due to its rodlike conformation and the lower binding constant of the $RuCE_5G$ complex may arise from partial charge compensation occurring between the oppositely charged portions of the metal peptide as they are brought closer together in the hairpin structure. These results demonstrated how gated ET experiments can be used to directly probe the dynamics of peptide−protein complexes and how apparently subtle changes made to the peptide sequence may produce large changes in the dynamics of the complexes that they form.

Design of a Cd(II)-Binding Site within the Interior of a Coiled-Coil Protein. The work from our group described above shows how de novo designed metalloproteins and metallopeptides can be used to study various aspects of biological ET reactions. However, it is noted that the design of these systems simply appended nonnative coordination complexes, such as ruthenium pentaammine and polypyridyl complexes, to the surfaces of these proteins in order to facilitate these reactions.[36,66,67] Consequently, the early ET metalloproteins studied by our group can be considered to be intrinsically abiotic in that they did not contain nativelike cofactors in which redox-active transition metals were directly coordinated to amino acid residues located within the hydrophobic core of these proteins, as is typically observed for many native systems. Thus, consideration was given toward devising ways of preparing more native-like ET metalloproteins through the incorporation of more native-like transition-metal cofactors into the interior of synthetic redox proteins. Once prepared, such functionally active de novo designed metalloproteins will provide a useful system in which to study how protein environments can be used to tune the chemical reactivity of embedded cofactors.

Recent efforts by our group have successfully incorporated a Cys-containing metal-binding site into the hydrophobic core

(65) Liu, L.; Hong, J.; Ogawa, M. Y. *J. Am. Chem. Soc.* **2004**, *126*, 50−51.
(66) Gray, H. B.; Winkler, J. R. *Q. Rev. Biophys.* **2003**, *36*, 341−372.
(67) Page, C. C.; Moser, C. C.; Dutton, P. L. *Curr. Opin. Chem. Biol.* **2003**, *7*, 551−556.

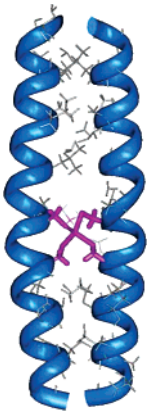

Figure 7. Energy-minimized computer model of the Cd-bridged C16C19 peptide dimer in which Cys residues located at postions 16 and 19 of each peptide chain bind the Cd center in a tetrahedral geometry.

of α-helical coiled-coils.[27] The peptide sequence employed in this study was based on the IEALEGK heptad repeat used by our group in the mechanistic ET studies described above.[36,46,48,51−53] However, here the peptide sequence was modified to contain the Cys-X-X-Cys metal-binding domain of rubredoxin in which four Cys residues create a tetrahedral coordination sphere for Fe^{2+}. The computer model shown in Figure 7 illustrates how the appropriate incorporation of the Cys-X-X-Cys tetrad into positions 16−19 of the coiled-coil sequence places Cys residues at the hydrophobic "a" and "d" positions of the third heptad repeat, which may result in the creation of a rubredoxin-like metal-binding site. Energy minimization calculations predict that binding of a Cd(II) ion to this site will result in dihedral bond angles ranging from 104.6° to 118.4° and Cd−S distances of ca. 2.55 Å, which are consistent with those observed for Cd-substituted desulforedoxins.[68] From these results, a 32-mer peptide called C16C19-GGY was prepared having the sequence

Ac-K(IEALEGK)$_2$(**C**EA**C**EGK)(IEALEGK)GGY-NH$_2$
C16C19-GGY

which places Cys residues at both the "a" and "d" positions of the third heptad repeat. The C16C19-GGY peptide was purified by reversed-phase HPLC and characterized by matrix-assisted laser desorption ionization mass spectroscopy. Figure 8 shows that the CD spectrum of C16C19-GGY consists of a large, negative maximum centered at 205 nm to indicate that the apopeptide exists as a disordered random coil in aqueous solution. This was an unexpected result based on our previous experience with similar peptides and shows that the substitution of Cys residues into the hydrophobic core disrupts the coiled-coil structure. Possible reasons for this include the introduction of different side-chain packing interactions into the hydrophobic core of the putative coiled-coil and/or the lowered hydrophobicity of the cysteinyl side chain. Importantly, the results presented in Figure 8 also show that the CD spectrum of the reduced C16C19-GGY peptide changes substantially upon the addition of $CdCl_2$. Negative maxima were then observed at 208 and 222 nm to indicate the presence of α helices. Further, the intensity of these signals increased with increasing amounts of Cd(II) added to the solution and yielded an ellipticity ratio of $[\theta_{222}]/[\theta_{208}] = 0.99$, which falls within the range generally regarded to indicate the presence of a coiled-coil structure.[57]

The aggregation state of the metal−peptide assembly was studied by HPSEC, which has been shown to be a reliable method for determining the oligomerization states of α-helical coiled-coils.[50] In these experiments, the elution profile of C16C19-GGY was obtained in both the absence and presence of Cd(II) and then compared with those of several peptide standards. The results indicate that the apopeptide has an apparent molecular mass of 3.3 kDa, which shows that it exists as a monomer. However, the behavior of the Cd−peptide yields an apparent molecular mass of 5.3 kDa, which indicates that the metalloprotein exists as a peptide dimer. These results show that the C16C19-GGY peptide undergoes a metal-induced folding process from a monomeric random coil to the organized structure of a two-stranded α-helical coiled-coil upon binding Cd(II). The metal−peptide stoichiometry of the dimeric peptide was studied by UV−vis spectroscopy because a UV absorption band at 238 nm is observed upon the addition of Cd(II) to a solution of C16C19. This band is assigned to the ligand-to-metal charge-transfer (LMCT) transition of the newly formed Cd−S bond.[69] A Job plot was constructed by measuring the absorbance at 238 nm as a function of the mole fraction of Cd(II) present in solution and demonstrated the existence of a 2:1 peptide−metal complex. These results were supported by spectrophotometric titrations in which the absorption intensity at 238 nm was seen to increase with successive additions of $CdCl_2$, reaching a limiting value at higher concentrations of added Cd(II) (Figure 9). As seen, the plot has a break at 0.5 equiv of Cd(II) added per peptide to further indicate the presence of a 2:1 peptide−metal complex.

In summary, the incorporation of the Cys-X-X-Cys metal-binding motif into the sequence of the C16C19-GGY apopeptide causes the peptide to exist as a monomeric random coil in free solution. However, the peptide then assembles into a metal-bridged coiled-coil dimer upon binding Cd(II). This behavior is reminiscent of that observed for the copper chaperone HAH1, which forms a metal-bridged dimer in the presence of Cu(I),[70,71] and for the related Cu-trafficking protein CopZ, whose metal-dependent dimerization was studied by electrospray ionization mass spectrometry,[72] analytical ultracentrifugation, and spectroscopic titrations.[73,74]

(68) Archer, M.; Carvalho, A. L.; Teixeira, S.; Moura, I.; Moura, J. J. G.; Rusnak, F.; Romao, M. J. *Protein Sci.* **1999**, *8*, 1536−1545.
(69) Henehan, C. J.; Pountney, D. L.; Zerbe, O.; Vasak, M. *Protein Sci.* **1993**, *2*, 1756−1764.
(70) Wernimont, A. K.; Huffman, D. L.; Lamb, A. L.; O'Halloran, T. V.; Rosenzweig, A. C. *Nat. Struct. Biol.* **2000**, *7*, 766−771.
(71) Tanchou, V.; Gas, F.; Urvoas, A.; Cougouluegne, F.; Ruat, S.; Averseng, O.; Quemeneur, E. *Biochem. Biophys. Res. Commun.* **2004**, *325*, 388−394.
(72) Urvoas, A.; Amekraz, B.; Moulin, C.; Le Clainche, L.; Stocklin, R.; Moutiez, M. *Rapid Commun. Mass Spectrom.* **2003**, *17*, 1889−1896.
(73) Urvoas, A.; Moutiez, M.; Estienne, C.; Couprie, J.; Mintz, E.; Le Clainche, L. *Eur. J. Biochem.* **2004**, *271*, 993−1003.
(74) Kihlken, M. A.; Leech, A. P.; Le Brun, N. E. *Biochem. J.* **2002**, *368*, 729−739.

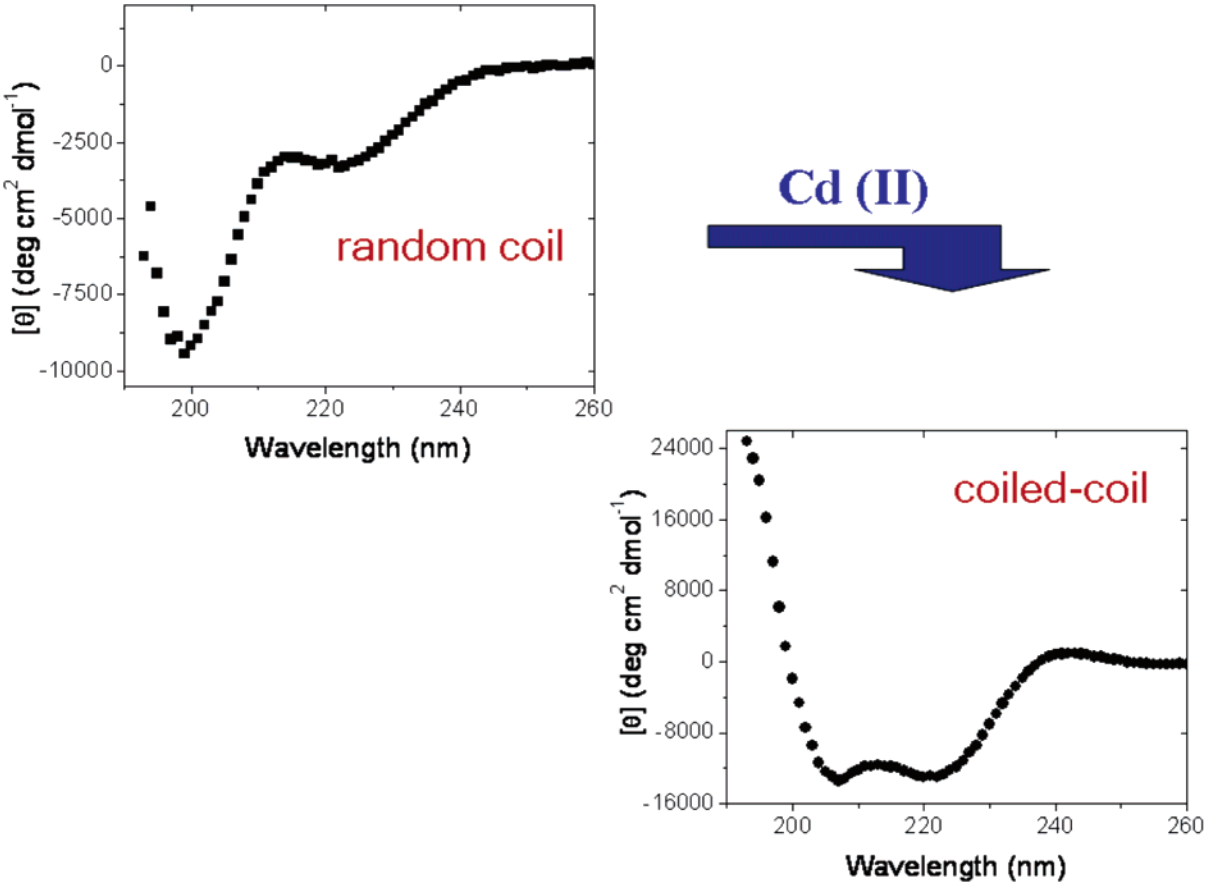

Figure 8. Changes in the CD spectrum of C16C19-GGY upon the addition of $CdCl_2$ to a 100 μM solution of C16C19-GGY containing the reducing agent tris(2-carboxyethyl)phosphine (TCEP; 100−200 μM) at pH 5.3 under deaerated conditions.

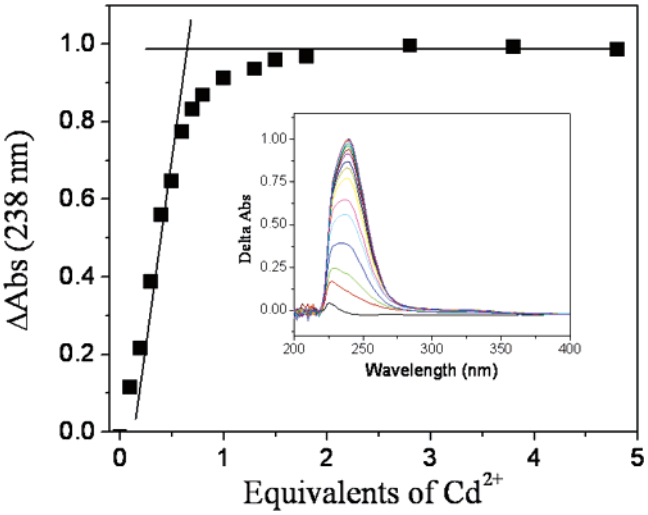

Figure 9. UV−vis titration in which successive additions of $CdCl_2$ were made to a 100 μM solution of C16C19-GGY containing the reducing agent TCEP (100−200 μM) in a 0.2 M acetate buffer (pH 5.4) under deaerated conditions.

Metal-Specific Protein-Folding Properties of C16C19-GGY. The observation that C16C19-GGY undergoes a Cd(II)-induced conformational change from a random coil to a two-stranded coiled-coil prompted further investigation of the metal-binding properties of this peptide.[75] New CD results show that the random-coil C16C19-GGY peptide monomer folds into an α-helical coiled-coil when in the presence of such soft metal ions as Hg(II), Cu(I), Au(I), and Ag(I) but continues to exist as a disordered random coil in the presence of Fe(II), Co(II), Ni(II), Zn(II), and Pb(II). The data presented in Table 1 show that binding of the various soft metal ions to C16C19-GGY results in a significant variation of the helical content of the resulting metalloproteins. Perhaps more dramatically, the oligomerization states of these different metalloproteins were determined by HPSEC and range in size from being peptide dimers for the Cd(II) and Hg(II) adducts to peptide hexamers for the Au(I)−protein. The binding of Cu(I) and Ag(I) to C16C19-GGY produces the intermediate case of peptide tetramers, which in the case of the Cu(I) adduct has been verified by analytical ultracentrifugation.[28] Interestingly, no obvious trend with

Table 1. Conformational Properties of Different Metal Adducts of C16C19-GGY

	Cd(II)	Hg(II)	Cu(I)	Ag(I)	Au(I)
$[\theta_{222}]/[\theta_{208}]^a$	0.99	1.15	0.97	1.13	1.04
$[\theta_{222}]^a$ (deg cm^2 dmol^{-1})	−16 400	−23 900	−21 300	−27 800	−10 200
oligomerization^b	dimer	dimer	tetramer	tetramer	hexamer

^{a} Measured upon the addition of equimolar amounts of metal ion ($CdCl_2$, $HgCl_2$, $[Cu(CH_3CN)_4]PF_6$, $AgNO_3$, and sodium aurothiomalate) and C16C19-GGY in sodium acetate buffer (pH 5.5). ^{b} Measured by HPSEC as described in the text.

(75) Kharenko, O. Ph.D. Dissertation, Bowling Green State University, Bowling Green, OH, 2005.

ionic radii is observed because binding of the largest ion in the series [Au(I)] is seen to form the largest peptide oligomer but the comparably sized Ag(I) and Hg(II) ions produce peptide tetramers and dimers, respectively. Thus, the binding of different metal ions to the C16C19-GGY peptides produces significant differences in the conformational properties of the resulting C16C19-GGY holoproteins. Interpreted within Pecoraro's TRI paradigm,[15] these results indicate that the C16C19-GGY peptide does not have a strong preference for a particular coiled-coil geometry and that the coordination properties of the different metal ions strongly influence the conformation of the resulting metalloprotein.

Binding of Cu(I) To Create a Luminescent Coiled-Coil Metalloprotein. Our studies of the Cu(I) adduct of C16C19-GGY led to the interesting observation of an intense (ϕ = 0.053) ambient temperature luminescence centered at 600 nm, which persists upon allowing the protein to stand overnight under ambient conditions.[28] It was found that this luminescence can be quenched by the addition of either ferricyanide, oxygen, or urea to respectively indicate that the emitting species is associated with the reduced Cu(I) state, has significant triplet character, and is quenched upon exposure to the bulk solvent. It is noteworthy that similar photoluminescent properties have been reported for Cu(I) derivatives of the Cys-rich metal-binding protein metallothionein[76,77] as well as the Cox17 copper chaperone[78] and the Cu-responsive transcription factors ACE1[79] and CopY,[80] all of which contain polynuclear Cu(I) clusters that are buried within the protein to shield them from the bulk solvent.[81] This is consistent with earlier studies of small-molecule copper(I) thiolate compounds in which luminescence is observed for polynuclear metal clusters where metal−metal interactions play an important role in stabilizing the emissive photoexcited state.[82] Thus, the observation of a 600-nm luminescence from Cu^{I}-C16C19-GGY suggests that it likely contains a polynuclear Cu(I) cluster.

The metal-binding stoichiometry of the Cu−protein was therefore determined by monitoring the various spectral changes that can be observed upon the addition of Cu(I). The data in Figure 10 show that the emission intensity of Cu^{I}-C16C19-GGY increases with increasing amounts of Cu(I) added to the solution of peptide but saturates after ca. 0.9 equiv of metal ion has been added. As with the oligomerization state of the Cu(I) adduct of C16C19-GGY, which exists as a peptide tetramer, this behavior is in marked contrast to that previously observed for the Cd(II)−protein and indicates that 4 equiv of Cu(I) is present in this new peptide tetramer. UV titrations were used to confirm these

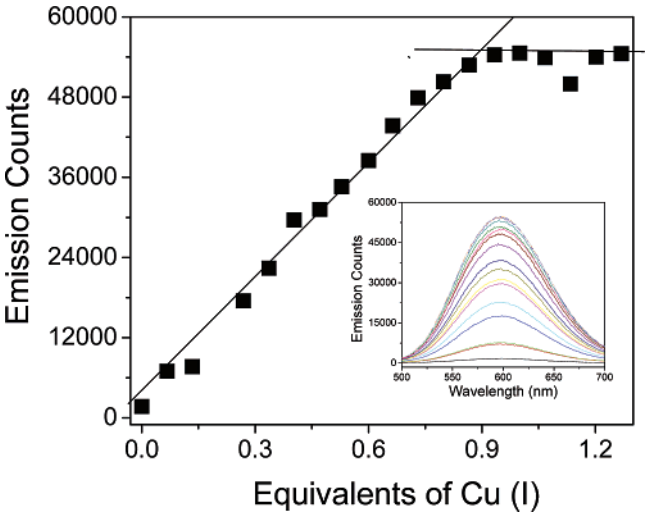

Figure 10. Emission titration of C16C19-GGY by $[Cu(CH_3CN)_4]PF_6$. Inset: Emission spectra obtained upon the addition of Cu(I) to the peptide solution. Conditions: 120 μM C16C19-GGY in a 0.2 M acetate buffer (pH 5.4) containing 730 μM TCEP as a reducing agent.

results because the binding of Cu(I) to Cys residues is known to produce both Cys−thiolate to Cu(I) LMCT and metal-centered (MC) transitions in the UV region of the spectrum.[83,84] Indeed, the addition of Cu(I) to a solution of C16C19-GGY does produce a new absorption band having a maximum at 236 nm and a shoulder at 296 nm. By analogy to studies of copper metallothionein, the lower energy absorption can be assigned to a clustered−centered transition whose intensity should be proportional to the number of bound metal ions and the higher energy band is likely due to the LMCT transition having an extinction coefficient of ca. 5500 M^{-1} cm^{-1} per metal−Cys bond.[83] The absorption at 296 nm does indeed increase with increasing amounts of added Cu(I), and saturates after 1 equiv of Cu has been added to confirm the 1:1 peptide−metal stoichiometry. The measured extinction coefficient at 236 nm further suggests the presence of 4.0 Cu(I)−Cys bonds in the metal cofactor.

The nature of the multinuclear Cu center was characterized by X-ray absorption spectroscopy.[28] The Cu K-edge X-ray absorption near-edge structure spectrum of Cu^{I}-C16C19-GGY showed the existence of Cu(I) ions having a trigonal coordination geometry, and extended X-ray absorption fine structure analysis suggested that each Cu(I) ion was surrounded by a ligand set consisting of one N/O and two S donors at average distances of 1.89(2) and 2.22(2) Å, respectively. The data also revealed the presence of additional scatterers in the second and third coordination sphere of the Cu centers, indicating the presence of a tetranuclear Cu cluster in which adjacent Cu(I) ions are bridged by the side chains of two Cys residues and each Cu atom also has a terminal N/O ligand. This model is consistent with the titration of free thiol groups with 5,5′-dithiobis(2-nitrobenzoic acid), which confirmed the presence of one free thiol group

(76) Gasyna, Z.; Zelazowski, A.; Green, A. R.; Ough, E.; Stillman, M. J. *Inorg. Chim. Acta* **1988**, *153*, 115−118.
(77) Green, A. R.; Stillman, M. J. *Inorg. Chim. Acta* **1994**, *226*, 275−283.
(78) Heaton, D. N.; George, G. N.; Garrison, G.; Winge, D. R. *Biochemistry* **2001**, *40*, 743−751.
(79) Casasfinet, J. R.; Hu, S.; Hamer, D.; Karpel, R. L. *Biochemistry* **1992**, *31*, 6617−6626.
(80) Cobine, P. A.; George, G. N.; Jones, C. E.; Wickramasinghe, W. A.; Solioz, M.; Dameron, C. T. *Biochemistry* **2002**, *41*, 5822−5829.
(81) Stillman, M. J. *Coord. Chem. Rev.* **1995**, *144*, 461−511.
(82) Ford, P. C.; Cariati, E.; Bourassa, J. *Chem. Rev.* **1999**, *99*, 3625−3647.
(83) Pountney, D. L.; Schauwecker, I.; Zarn, J.; Vasak, M. *Biochemistry* **1994**, *33*, 9699−9705.
(84) Bogumil, R.; Faller, P.; Pountney, D. L.; Vasak, M. *Eur. J. Biochem.* **1996**, *238*, 698−705.

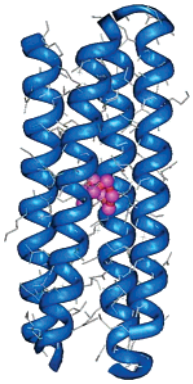

Figure 11. Computer-generated model of the tetrameric Cu^{I}-C16C19-GGY metalloprotein.

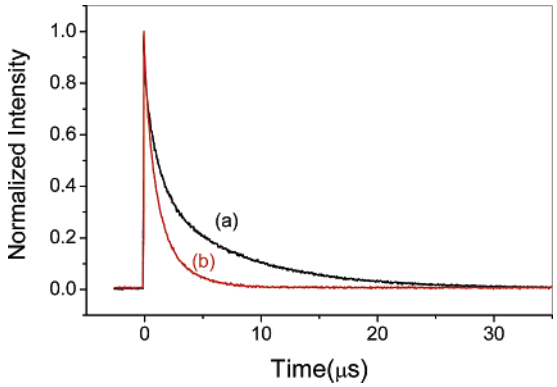

Figure 12. Emission lifetime of 25 μM Cu^{I}-C16C19-GGY taken in the (a) absence and (b) presence of 100 μM $[Ru(NH_3)_5Py]^{3+}$ in a 0.2 M acetate buffer (pH 5.4). The solid lines are the fits to eq 1 where for trace (a) $k_S = 9.5 \times 10^5\ s^{-1}$, $k_L = 1.3 \times 10^5\ s^{-1}$, and $A_S/A_L = 1$ and for trace (b) $k_S = 1.1 \times 10^6\ s^{-1}$, $k_L = 4.2 \times 10^5\ s^{-1}$, and $A_S/A_L = 1$.

per peptide chain in the metalloprotein. Figure 11 shows a likely model of Cu^{I}-C16C19-GGY.

Photoinduced ET Involving the Cu^{I}-C16C19-GGY Metalloprotein. The strong room temperature luminescence of Cu^{I}-C16C19-GGY suggests that it might function as a photoinduced ET protein, which can be monitored by emission-lifetime experiments. As a control, Figure 12 shows that the emission lifetime of this species can be accurately fit to double-exponential decay kinetics (eq 1), in which A_S, k_S and A_L, k_L are the amplitudes and rate constants of the

$$I(t) = A_S \exp(-k_S t) + A_L \exp(-k_L t) \qquad (1)$$

shorter and longer lifetime components, respectively. A nonlinear least-squares fit of the data yields values of $k_S = 9.5 \times 10^5\ s^{-1}$ ($\tau_S = 1.1\ \mu s$), $k_L = 1.3 \times 10^5\ s^{-1}$ ($\tau_L = 7.7\ \mu s$), and $A_S/A_L = 1$, where τ_L and τ_S are the emission lifetimes of their respective components. These results suggest that the $Cu^{I}_4S_4(N/O)_4$ cofactor of Cu^{I}-C16C19-GGY contains two independent lumophores, and it is speculated that the two emissive sites of this protein might be due to the presence of two electronically independent Cu(I)−Cu(I) dimers located within the $Cu^{I}_4S_4(N/O)_4$ cofactor. However, additional explanations for this cannot be ruled out at this time.

Importantly, the data shown in Figure 12 also show that both lifetime components of this protein are quenched in the presence of the electron acceptor $[Ru(NH_3)_5Py]^{3+}$ where Py = pyridine, and it has been shown that this behavior is accompanied by an increased absorption at 400 nm to indicate the formation of the reduced $[Ru(NH_3)_5Py]^{2+}$ quencher in a photoinduced ET event. It is further noted that the relative amplitudes of the fast and slow emission decay components remain approximately equal at all quencher concentrations studied and that plots of the observed emission decay constants k_S^{obs} and k_L^{obs} are linearly dependent upon the concentration of the quencher because pseudo-first-order quenching kinetics are observed (Figure 13). Analysis of the data yields values for the bimolecular quenching constants of $k_S^{ET} = (2.46 \pm 0.07) \times 10^9\ M^{-1}\ s^{-1}$ and $k_L^{ET} = (1.36 \pm 0.05) \times 10^9\ M^{-1}\ s^{-1}$, respectively. Together, these results show that the luminescent polynuclear Cu center in the synthetic metalloprotein Cu^{I}-C16C19-GGY can indeed function as a photoinduced ET protein by undergoing a bimolecular reaction with an exogenous acceptor in free solution.

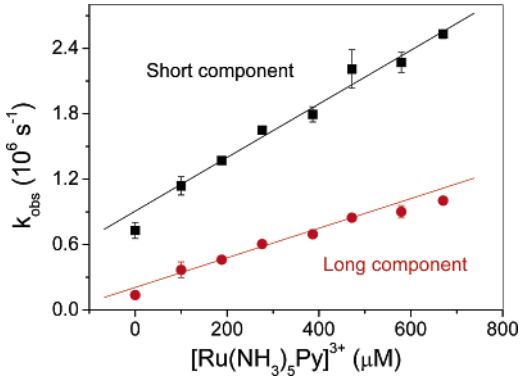

Figure 13. Observed emission decay rate constants for the long- and short-lived emission components of Cu^{I}-C16C19-GGY (ca. 25 μM) taken as a function of the concentration of added $[Ru(NH_3)_5Py]^{3+}$ in a 0.2 M acetate buffer (pH 5.4). The error bars are the deviation from the mean of triplicate experiments.

Conclusion

In conclusion, the α-helical coiled-coil motif has served as a robust scaffold for constructing synthetic ET metalloproteins. Early work from our group appended exogenous, and abiotic, Ru-based redox centers to the solvent-exposed surfaces of these proteins for intramolecular ET studies. Recent work involved the incorporation of a more nativelike Cu(I) redox center into the hydrophobic interior of a synthetic protein. This work showed how the structures of the resulting metalloproteins are controlled by the subtle interplay between the directional bonding properties of their inorganic cofactors and those of their protein environments. Future work from our laboratory will continue to examine how the conformational and chemical (i.e., ET) properties of these model proteins can be controlled by these factors. It is hoped that knowledge gained from this work will contribute to the expanding effort of bioinorganic chemists to prepare new kinds of functionally active synthetic metalloproteins.

Note Added in Proof: During the editing of this manuscript our group completed a study of the driving force dependence of the rates of photoinduced ET occurring between Cu^{I}-C16C19-GGY and a series of ruthenium am-

mine acceptors. The results provide evidence for inverted Marcus behavior in these collisional charge separation reactions. (Hong, J.; Kharenko, O. A.; Petros, A. K.; Gibney, B. R.; Ogawa, M. Y. *Angew. Chem., Int. Ed.* **2006**, *37*, 6137−6140).

Acknowledgment. The authors thank Mikhail Tsurkan, Xianchun Zhu, Fei Xie, Elena Ptchelnikova, and Jiufeng Fan for help in preparing this manuscript. The Ohio Laboratory for Kinetic Spectrometry and Profs. M. A. J. Rodgers and F. Castellano are thanked for use of the laser facilities. This work was sponsored by NIH Grant GM61171, NSF Grant CHE-0455441, and ACS-PRF 34901-AC.

IC060222J